Clinical Infectious Diseases

MAJOR ARTICLE

Altered Maternal Antibody Profiles in Women With Human Immunodeficiency Virus Drive Changes in Transplacental Antibody Transfer

Sepideh Dolatshahi,[1] Audrey L. Butler,[2] Mark J. Siedner,[3,4,5] Joseph Ngonzi,[6] Andrea G. Edlow,[7] Julian Adong,[6] Madeleine F. Jennewein,[8] Caroline Atyeo,[9] Ingrid V. Bassett,[3,4] Drucilla J. Roberts,[10] Douglas A. Lauffenburger,[11] Galit Alter,[3,9,a] and Lisa M. Bebell[3,4,5,a]

[1]Department of Biomedical Engineering, University of Virginia, Charlottesville, Virginia, USA; [2]State University of New York Upstate Medical University, Syracuse, New York, USA; [3]Division of Infectious Diseases, Massachusetts General Hospital, Boston, Massachusetts, USA; [4]Medical Practice Evaluation Center, Massachusetts General Hospital, Boston, Massachusetts, USA; [5]Center for Global Health, Massachusetts General Hospital, Boston, Massachusetts, USA; [6]Mbarara University of Science and Technology, Mbarara, Uganda; [7]Division of Maternal-Fetal Medicine, Department of Obstetrics and Gynecology, Massachusetts General Hospital, Boston, Massachusetts, USA; [8]Fred Hutchinson Cancer Center, Seattle, Washington, USA; [9]Ragon Institute of Massachusetts General Hospital, Massachusetts Institute of Technology and Harvard, Cambridge, Massachusetts, USA; [10]Department of Pathology, Massachusetts General Hospital, Boston, Massachusetts, USA; and [11]Massachusetts Institute of Technology, Cambridge, Massachusetts, USA

Background. Human immunodeficiency virus (HIV)–exposed, uninfected (HEU) children have a higher risk of severe infection, but the causes are poorly understood. Emerging data point to altered antibody transfer in women with HIV (WHIV); however, specific perturbations and the influence of antiretroviral therapy (ART) and HIV viremia remain unclear.

Methods. We evaluated antigen-specific transplacental antibody transfer across 14 antigens in paired maternal and umbilical cord plasma from 352 Ugandan women; 176 were WHIV taking ART. We measured antigen-specific immunoglobulin G (IgG) subclass (IgG1, 2, 3, 4) levels and antibody Fcγ receptor (FcγRn, 2a, 2b, 3a, 3b) binding profiles. We used partial least squares discriminant analysis to define antigen-specific transplacental antibody transfer features.

Results. Global antibody transfer patterns were similar by maternal HIV serostatus, pointing to effective placental function in WHIV. However, HEU umbilical cord antibody profiles were altered, driven by perturbed WHIV seroprofiles, with higher levels of herpesvirus antibodies ($P < .01$ for Epstein-Barr virus, herpes simplex virus) and lower levels of classic vaccine-induced antibodies ($P < .01$ for tetanus, polio, *Haemophilus influenzae* type b), suggesting that umbilical cord antibody profile differences arise from imbalanced WHIV immunity. Abnormal WHIV antibody profiles were associated with HIV viremia, lower CD4 count, and postconception ART initiation ($P = .01$).

Conclusions. Perturbed immune-dominance profiles in WHIV shift the balance of immunity delivered to neonates. Perturbed HIV-associated maternal antibody profiles are a key determinant of compromised neonatal immunity. Maternal vaccination interventions may promote transfer of relevant, effective antibodies to protect HEU children against early-life infections.

Keywords. immunity; neonate; placenta; Africa; vertical.

Mother-to-child HIV transmission prevention programs have markedly decreased the global incidence of vertically transmitted human immunodeficiency virus (HIV). Yet, >1 million HIV-exposed, uninfected (HEU) children are born annually and have a higher risk of severe infections [1, 2] and infection-related hospitalization than HIV-unexposed children [2, 3]. In the current era of widespread maternal antiretroviral therapy (ART), the causes of increased infection risk and severity among HEU infants are poorly understood [4], though altered transplacental antibody transfer could increase susceptibility. Prior studies reported both compromised and unchanged total and antigen-specific immunoglobulin G (IgG) transplacental antibody transfer ratios in women with HIV (WHIV) [5–8].

Immunity in WHIV may be negatively impacted by HIV viremia, low $CD4^+$ T-cell (CD4) count, and suboptimal ART efficacy or adherence [5–8]. Furthermore, late ART initiation in pregnancy, nonadherence, or treatment interruptions may hinder maternal immune reconstitution, drive HIV viremia, alter maternal humoral and cellular immunity in pregnant WHIV, and inhibit vaccine responsiveness. However, the plasma antibody repertoire in WHIV taking ART has not been comprehensively evaluated, nor has it been established whether global placental antibody transfer is compromised in WHIV and whether function can be restored with ART. Thus, drivers of altered HEU neonate immunity remain ill-defined, including how maternal antibody profiles contribute to compromised immunity.

Prior to widespread ART, placental abnormalities were more prevalent in WHIV [9–12]. Impaired transplacental IgG transfer

Received 2 October 2021; editorial decision 18 February 2022; published online 4 March 2022.
[a]G. A. and L. M. B. contributed equally to this work.
Correspondence: L. M. Bebell, Massachusetts General Hospital, Division of Infectious Diseases, GRJ-504, 55 Fruit St, Boston, MA 02114 (lbebell@mgh.harvard.edu).

Clinical Infectious Diseases® 2022;75(8):1359–69

https://doi.org/10.1093/cid/ciac156

in WHIV was associated with placental pathology and thought to be driven by placental inflammation [13, 14]. However, we previously found no significant difference in prevalence of inflammatory or vascular placental pathology by maternal HIV serostatus [15, 16], suggesting that antibody transfer perturbations originate outside the placenta and might be linked to altered maternal humoral immunity.

Thus, given lack of significant HIV-associated placental abnormalities in the ART era, we sought to examine maternal plasma antibody profiles in WHIV and impact on transplacental transfer. We used a systems serology approach to comprehensively profile maternal and umbilical cord antibodies to 14 vaccine-preventable and endemic antigens including antigen-specific isotype, subclass, and Fc receptor (FcR) binding levels by maternal HIV serostatus in a large cohort of 352 women living in sub-Saharan Africa, half of whom were WHIV.

MATERIALS AND METHODS

Study Site, Recruitment, and Ethics

Participants were recruited from Mbarara Regional Referral Hospital in 2017–2018. HIV-infected women who reported not taking ART were excluded. The study was approved by Mbarara University of Science and Technology (11/03-17) and Partners Healthcare (2017P001319).

Sample Collection

Maternal blood was collected during labor. HIV viral load and CD4 count were measured for WHIV if not available within the last 6 months. Umbilical vein and maternal blood was spun to separate plasma.

Antigen-Specific Antibody Isotype, Subclass, FcR Binding, and Enzyme-Linked Immunosorbent Assays

Measles, mumps, rubella, combined herpes simplex 1 and 2 (HSV-1/2), tetanus toxoid (tetanus), pertussis toxin (pertussis), poliovirus (polio), hepatitis A (HepA), cytomegalovirus (CMV), Epstein-Barr virus (EBV), respiratory syncytial virus (RSV), *Haemophilus influenzae* type b (Hib), adenovirus type 5 hexon, and purified protein derivative (PPD)–associated antigens were coupled to MagPlex microspheres via a 2-step carbodiimide reaction. Antigen-specific IgG subclass 1, 2, 3, and 4 assays were performed in duplicate, measured using Luminex assays, and read using Intellicyt iQue, as previously described [17]. Antigen-specific antibody binding assays to FcRγ2a, 2b, 3a, 3b, and FcRn were performed in duplicate, measured via Luminex as previously described [18]. Total IgG was measured by enzyme-linked immunosorbent assay according to the manufacturer's instructions (Invitrogen, 88-50550-22), reported as an average of duplicate wells.

Data Analysis and Visualization

Cohort characteristics were described using summary statistics. Antibody transfer ratios were calculated as paired ratio of umbilical cord:maternal antigen-specific absolute values for each subclass and receptor. Significance between groups was determined using Kruskal-Wallis tests, corrected for multiple comparisons using Dunn test.

Identifying Group-Specific Signatures: Least Absolute Shrinkage and Selection Operator, Orthogonalized Partial Least Squares Discriminant Analysis, and Co-correlate Networks

To identify antibody Fc features differentiating groups, classification models were built using a least absolute shrinkage and selection operator (LASSO) method for feature selection followed by classification using a nested cross-validation framework as previously described [19]. Orthogonalized partial least squares discriminant analysis (OPLSDA) was used to visualize LASSO-selected features [20]. For OPLSDA, variables were centered and scaled to a standard deviation of 1.0 (z score) and the model was orthogonalized so latent variable 1 (LV1) captured feature variance in pairwise separation of groups and latent variable 2 (LV2) described variance orthogonal (not contributing) to LV1. One hundred random 5-fold cross-validation and permutation testing was performed to assess model significance by randomly shuffling labels. The OPLSDA model performed significantly better than random with cross-validation Wilcoxon P values $\leq 10^{-8}$ across pairwise group comparisons. A score plot and a bar plot of loadings on LV1 were generated for each analysis to identify individual features capturing the greatest variance. Variable importance in projection (VIP) scores were calculated [21], ranking variable importance. Features were ranked by VIP score order and plotted according to the direction and group of enrichment. To comprehensively profile features differentiating groups, Fc features correlated to each LASSO-selected feature in the final models were identified and included in the Cytoscape correlation network depiction if (1) statistically significant after correction for multiple comparisons (Benjamini-Hochberg Q value <.05) and (2) correlation coefficient ≥0.3.

Multilevel Partial Least Squares Discriminant Analysis for Paired Multivariate Analysis

Multilevel partial least squares discriminant analysis (MLPLSDA) using LASSO-selected features and IgG subclass titers was used to identify key features contributing to the separation of paired maternal and umbilical cord plasma antibody Fc profiles [22, 23]. MLPLSDA is a multivariable method taking advantage of paired data structure by subtracting interpair variability to highlight intrapair variability [20]. Preprocessing and goodness-of-fit assessment was done similarly to OPLSDA.

Defining Multivariate Signatures

Orthogonalized partial least squares regression (OPLSR) modeling was used to define multivariate signatures for continuous variables, including maternal total IgG, total IgG transfer ratios, and HIV viral load. Input variables were scaled to zero mean and unit variance, and 100 permutations were performed in a 5-fold cross-validation framework, comparing permutation residuals to original residuals, reporting mean Wilcoxon *P* value over 100 iterations.

Three-Way Partial Least Squares Discriminant Analysis Model

Twelve LASSO-selected features from the 3 pairwise group comparisons (HIV uninfected, WHIV nonviremic [undetectable maternal HIV viral load <50 copies/mL], and WHIV viremic [maternal HIV viral load >50 copies/mL]) were pooled. A nonorthogonalized partial least squares discriminant analysis (PLSDA) model was developed to separate the 3 groups and better visualize pairwise group differences. Two-dimensional LV1 and LV2 loadings were overlaid to visualize the contributions of the 12 features to pairwise group differences in the resulting biplot.

RESULTS

Cohort Characteristics

Of 352 participants (Table 1), 176 (50%) were WHIV who reported taking combination ART. Demographics and obstetric history were similar by maternal HIV serostatus. Mean parity was 3.1, and mean gestational age was 39 weeks. Among WHIV, median CD4 count was 440 cells/μL, 74% had an undetectable HIV viral load, and 53% initiated ART preconception. Median ART days for those initiating postconception was 109.

Global Patterns of Antibody Transfer Were Similar by Maternal HIV Serostatus

To investigate transplacental IgG transfer, we compared the logarithm of antibody subclass transfer ratios by maternal HIV serostatus. Heatmap depiction of log IgG subclass transfer ratios (Figure 1A) demonstrated overall transfer landscape by serostatus. Because IgG1 followed by IgG4 and IgG3 are preferentially transplacentally transferred (ratio >1) [24, 25], we visualized these subclass ratios by maternal HIV serostatus using radar plots (Figure 1B). We observed striking stability across most antigen specificities, with small but statistically significant lower IgG1 transfer ratios in WHIV for RSV ($P = .029$) and HSV-1/2 ($P = .0008$). IgG2 and IgG3 transfer ratios were significantly lower in WHIV for Hib, rubella, HSV-1/2, and EBV (Supplementary Figure 1*A* and 1*B*). IgG1 transfer ratio distribution was visualized using violin plots, demonstrating similar spread of ratios across antigens by maternal HIV serostatus (Figure 1C).

Given few univariate antigen-specific differences and similar, stable overall transfer ratios, we investigated whether multivariate transfer patterns differed by maternal HIV serostatus. Using unbiased MLPLSDA analyses of IgG subclass titers to discriminate across mother:umbilical cord pairs, top features contributing to IgG separation included IgG1 for polio and PPD, which were more abundant in umbilical cord than maternal plasma for both HIV serogroups (Supplementary Figure 1*H–K*). IgG2 for polio and CMV and IgG4 for mumps and measles demonstrated the opposite pattern, with higher maternal than umbilical cord levels. Results were similar with and without LASSO feature reduction, indicating overall similar transplacental IgG transfer patterns by maternal HIV serostatus, despite significant small decreases in individual subclass ratios in WHIV. Together,

Table 1. Cohort Characteristics

Characteristic	Living With HIV (n = 176)	HIV Uninfected (n = 176)	*P* Value[a]
Age category, y			.38
≤19	11 (6)	18 (10)	
20–34	139 (79)	135 (77)	
≥35	26 (15)	23 (13)	
Gestational age, wk, mean (SD)	39 (2.1)	39 (1.7)	.47
Parity prior to current delivery			.07
0 (primiparous)	30 (17)	46 (26)	
1–3 (multiparous)	109 (62)	90 (51)	
>4 (grand multiparous)	37 (21)	40 (23)	
Cesarean delivery	66 (38)	48 (27)	.04
Presence of CPI	16 (9)	12 (14)	.18
Villitis of unknown etiology	8 (5)	18 (10)	.04
Plasma cell deciduitis	7 (4)	5 (3)	.82
Chronic chorioamnionitis	1 (0.6)	3 (2)	.37
Chronic histiocytic intervillositis	0 (0)	0 (0)	

Data are presented as No. (%) unless otherwise indicated.

Abbreviations: CPI, chronic placental inflammation; HIV, human immunodeficiency virus; SD, standard deviation.

[a]Tests of association between cohort characteristics and HIV serostatus were performed using χ^2, Wilcoxon rank-sum, and *t* tests.

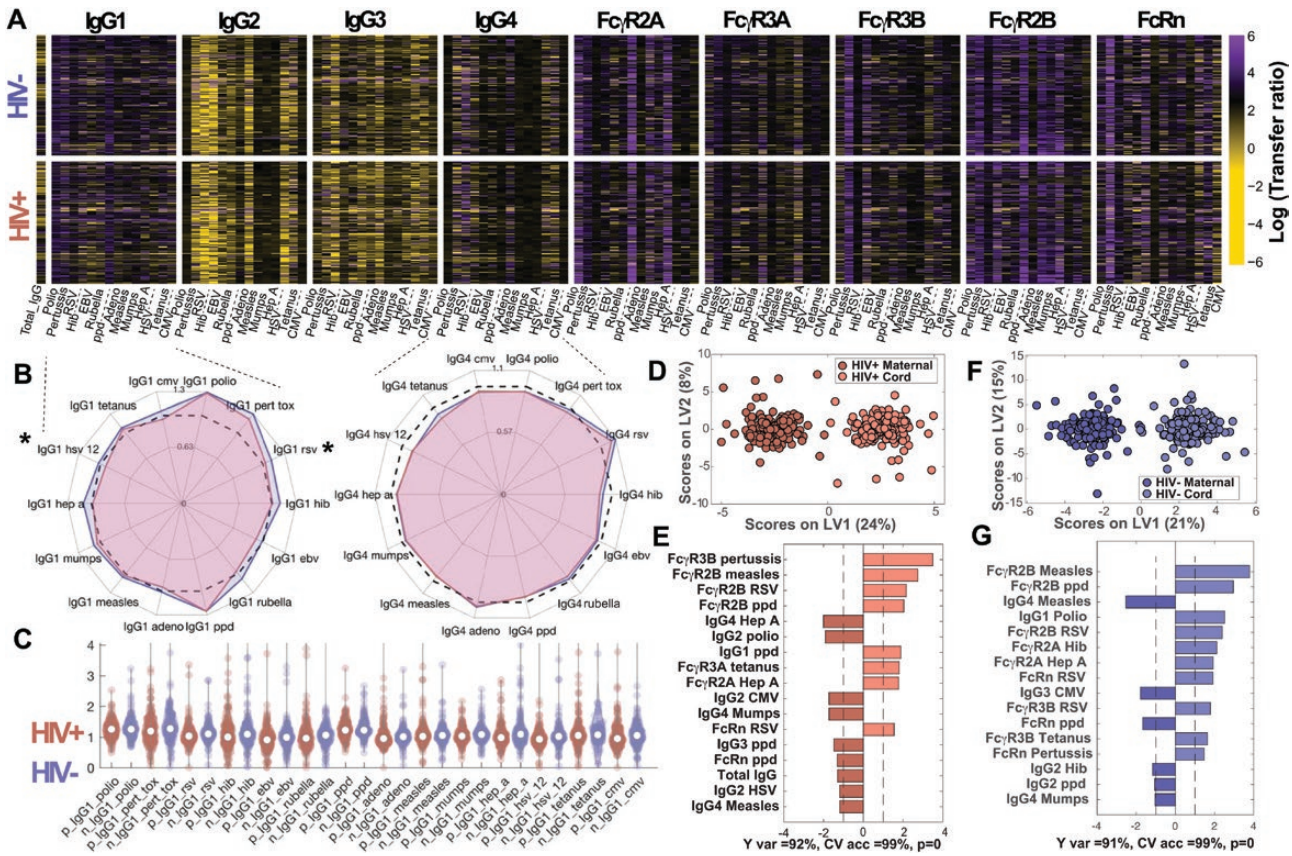

Figure 1. Global patterns of antibody transfer were similar between women with human immunodeficiency virus (WHIV) and human immunodeficiency virus (HIV)–uninfected women. This figure depicts the global antibody pool and transplacental transfer patterns across HIV-positive and HIV-negative pregnancies (*A–C*) and multivariate analysis distinguishing maternal and umbilical cord antibody profiles (*D–G*). *A*, Transplacental transfer ratios. Heatmap depicting the logarithm of transfer ratios (umbilical cord plasma level divided by maternal plasma level). Colors depict transfer ratios: black = 1, purple >1, and yellow <1. *B*, Median transfer ratios for highly transferred immunoglobulin G1 (IgG1) and immunoglobulin G4 (IgG4), comparing HIV-positive to HIV-negative pregnancies. Radar plots show median antigen-specific IgG1 and IgG4 transfer ratios for WHIV (red) and HIV-uninfected women (blue). The dashed black line represents transfer ratio = 1. Mann-Whitney *U* test was used to test the hypothesis that transfer ratios were sampled from continuous distributions with equal medians. *P* values were adjusted for multiple comparisons using Bonferroni correction for the 14 antigen specificities. *Significant corrected *P* values <.05. *C*, Distributions of transplacental antibody transfer ratios, depicted for WHIV and HIV-uninfected women using Violin plots. D–G, Multilevel OPLSDA models using 36 LASSO-selected features separating plasma profiles from WHIV and paired HIV-exposed umbilical cord plasma (*D* and *E*) and HIV-uninfected women and paired HIV-unexposed umbilical cord plasma (*F* and *G*), accounting for variance across maternal-cord pairs. *D*, Score plot, where dots represent maternal (darker color) and paired umbilical cord (lighter color) samples. The orthogonalized approach ensures that latent variable 1 (LV1) defines the axis of separation between mother and cord Fc profiles (Y var = 92% and X var = 24%), while latent variable 2 (LV2) captured the variance in the antibody profiles that do not contribute to this separation (Y var = 0% and X var = 8%). To assess model performance 5-fold cross-validation was performed, resulting in almost perfect accuracy (CV accuracy = 99%). *E*, Bar graph demonstrating the variable importance in projection (VIP) scores for the top features contributing most to the separation (VIP score >1). The VIP scores shown are ranked and color-coded according to the direction of the loadings and groups are color-matched to the score plot. *F*, Score plot, where dots represent maternal (darker color) and paired umbilical cord (lighter color) samples. The variance in mother:umbilical cord separation is condensed in LV1 (Y var = 91% and X var = 21%). LV2 captures the variance not contributing to the separation (Y var = 0% and X var = 15%). *G*, Bar graph demonstrating the VIP scores for the top features contributing most to separation. The VIP scores shown are ranked and color-coded according to the direction of the loadings and groups are color-matched to the score plot. Abbreviations: adeno, adenovirus; CMV, cytomegalovirus; CV acc, cross-validation accuracy; EBV, Epstein-Barr virus; FcR, Fc receptor; HepA, hepatitis A; Hib, *Haemophilus influenzae* type b; HIV, human immunodeficiency virus; IgG, immunoglobulin G; LV, latent variable; pert tox, pertussis toxin; RSV, respiratory syncytial virus.

despite a few small differences in transfer ratios driven by differences in maternal plasma levels, these data suggested intact placental antibody transfer functions in WHIV.

Beyond antibody levels, antibody function directed by pathogen-specific interaction with FcRs further protects against pathogens [26, 27]. We next investigated whether transferred antibodies differed by FcR-binding profiles. MLPLSDA of LASSO-selected features resulted in near-perfect separation by key Fc signatures with 99% cross-validation (CV) accuracy for both HIV serogroups (Figure 1D and 1F). The highest-ranking features separating maternal and umbilical cord profiles included measles-specific and RSV-specific FcγR2b, higher in umbilical cord than maternal plasma (Figure 1E and 1G). Our findings of similar IgG subclass ratios, FcR profiles, and top-ranking MLPLSDA-selected features suggest that placental antibody transfer functions remain largely intact among WHIV taking ART, and differences in umbilical cord blood seroprofiles originate outside the placenta and are likely due to maternal factors.

Differences in HIV-Exposed and -Unexposed Umbilical Cord Antibody Profiles Are Driven by Maternal Antibody Profiles

The surprising observation of largely similar transplacental transfer ratios across maternal HIV serogroups suggested that compromised HEU immunity may result from altered maternal plasma seroprofiles rather than placental dysfunction. We therefore analyzed maternal antibody profiles by HIV serostatus in univariate analysis, classified by inoculation route and pathogen type (Figure 2A–C). Compared to HIV-uninfected women, higher plasma levels of herpesvirus antibodies (herpesviruses latent in the host that can reactivate: HSV-1/2, EBV, CMV) were transferred to umbilical cord plasma in WHIV (Figure 2A). Opposite trends were observed with classic vaccine-induced antibodies to tetanus, Hib, mumps, and polio, with lower plasma levels among WHIV and resulting lower abundance in HEU umbilical cord plasma (Figure 2C). Other antigen-specific antibodies appeared unaffected by maternal HIV infection (Figure 2B). Maternal antibody levels were most predictive of transplacental antibody quantity transferred across the placenta, as seen previously [25]. Furthermore, maternal HIV infection was associated with higher maternal and umbilical cord levels of chronic herpesvirus antibodies, which likely outcompete antibodies to important childhood pathogens for transplacental transfer, resulting in lower umbilical cord levels and skewing HEU immunity away from optimal humoral protection (Figure 2C).

Next, we further defined umbilical cord plasma features by maternal HIV serostatus using LASSO-selected features in OPLSDA. Score plots (Figure 2D) depicted moderate (CV accuracy = 68%) but stable (permutation $P < 10^{-8}$) global profile differences. Higher EBV- and HSV-1/2–specific antibody titers and associated Fcγ receptors were associated with HIV-exposed umbilical cord plasma, while tetanus-, Hib-, and mumps-specific antibody titers and their Fcγ receptors were higher in the HIV-unexposed group (Figure 2E and 2F). Corresponding maternal plasma analysis demonstrated a similar pattern (Figure 2G–I), further suggesting that umbilical cord plasma antibody profile differences arise from imbalanced WHIV immunity—shifted away from vaccine-derived antigens and toward chronic viral pathogens. To delineate additional antibody features tracking with altered WHIV antibody profiles, we constructed a network of features significantly correlated to LASSO-selected features (Figure 2F and 2I). Hib-specific IgG1 and FcR-binding antibodies were highly correlated with LASSO-selected tetanus-specific FcRn binding (Figure 2F and 2I). To confirm that maternal differences determined profiles in paired umbilical cord plasma, we performed OPLSDA on LASSO-selected IgG1 features. Antigen-specific antibody differences were conserved, and EBV, HSV-1/2, tetanus, and Hib IgG1 titers were top-ranking differences by maternal HIV serostatus (Supplementary Figure 2). Collectively, our findings illustrate preserved placental antibody transfer function, and that altered maternal immune profiles in WHIV were the critical determinant of umbilical cord antibody levels.

Among WHIV, lower CD4 count, postconception ART initiation, and HIV viremia determine maternal plasma profiles, driving transplacental IgG transfer. Because HIV infection has been associated with hypergammaglobulinemia and poor placental antibody transfer [28], we investigated WHIV seroprofile determinants. Total IgG was significantly higher in WHIV than in HIV-uninfected women (Figure 3A; $P = .001$) but not significantly higher in HIV-exposed than in HIV-unexposed umbilical cord plasma (Figure 3A; $P = .4$). Using multivariate OPLSR, HIV viral load, lower CD4 count, and postconception ART initiation were tightly linked to high total maternal IgG levels (Figure 3B and 3C). A second OPLSR model defined lower maternal HIV viral load and higher CD4 count as top-ranking features associated with high total IgG transfer ratios (Figure 3D and 3E). Thus, maternal HIV viremia, lower CD4 count, and postconception ART initiation predicted total maternal IgG level and inversely predicted transplacental total IgG transfer ratio.

We then investigated the contribution of maternal HIV viremia and CD4 count to WHIV seroprofiles by comparing median antigen-specific IgG1 transplacental transfer ratios using radar plots (Figure 3F–H). Transfer ratios in viremic WHIV were almost universally lower than nonviremic WHIV, whose ratios were lower than HIV-uninfected women. Comparing viremic WHIV and HIV-uninfected women, we observed significantly decreased median transfer ratios for HepA-, HSV-1/2–, adenovirus-, and rubella-specific IgG1 (Figure 3F). WHIV with low CD4 counts (<250 cells/μL) had the lowest transfer ratios across all 14 antigens. Transfer efficiency was significantly different between low CD4 count in WHIV and HIV-uninfected women for polio-, rubella-, PPD-, and CMV-specific antibodies (Figure 3G). Timing of ART initiation also impacted transfer efficiency. Median transfer ratios were significantly lower in WHIV starting ART postconception than in HIV-uninfected women for HepA-, RSV-, and HSV-specific IgG1. Transfer ratios for WHIV who started ART preconception ranked between these 2 groups (Figure 3H). Thus, WHIV initiating ART preconception who achieved robust immune reconstitution demonstrated transplacental antibody transfer more similar to HIV-uninfected women than WHIV initiating ART postconception or with lower CD4 counts.

HIV Viremia Is Associated With Perturbed Maternal Seroprofiles

All enrolled WHIV reported taking ART, yet 26% had detectable HIV viremia. Using OPLSR, total IgG was the highest-ranking feature associated with HIV viral load (Figure 4A and 4B). We compared median maternal and umbilical cord IgG titers and transfer ratios for 131 (74%) nonviremic WHIV to 45 (26%) viremic WHIV and 176 HIV-uninfected women. Maternal total IgG levels were significantly higher

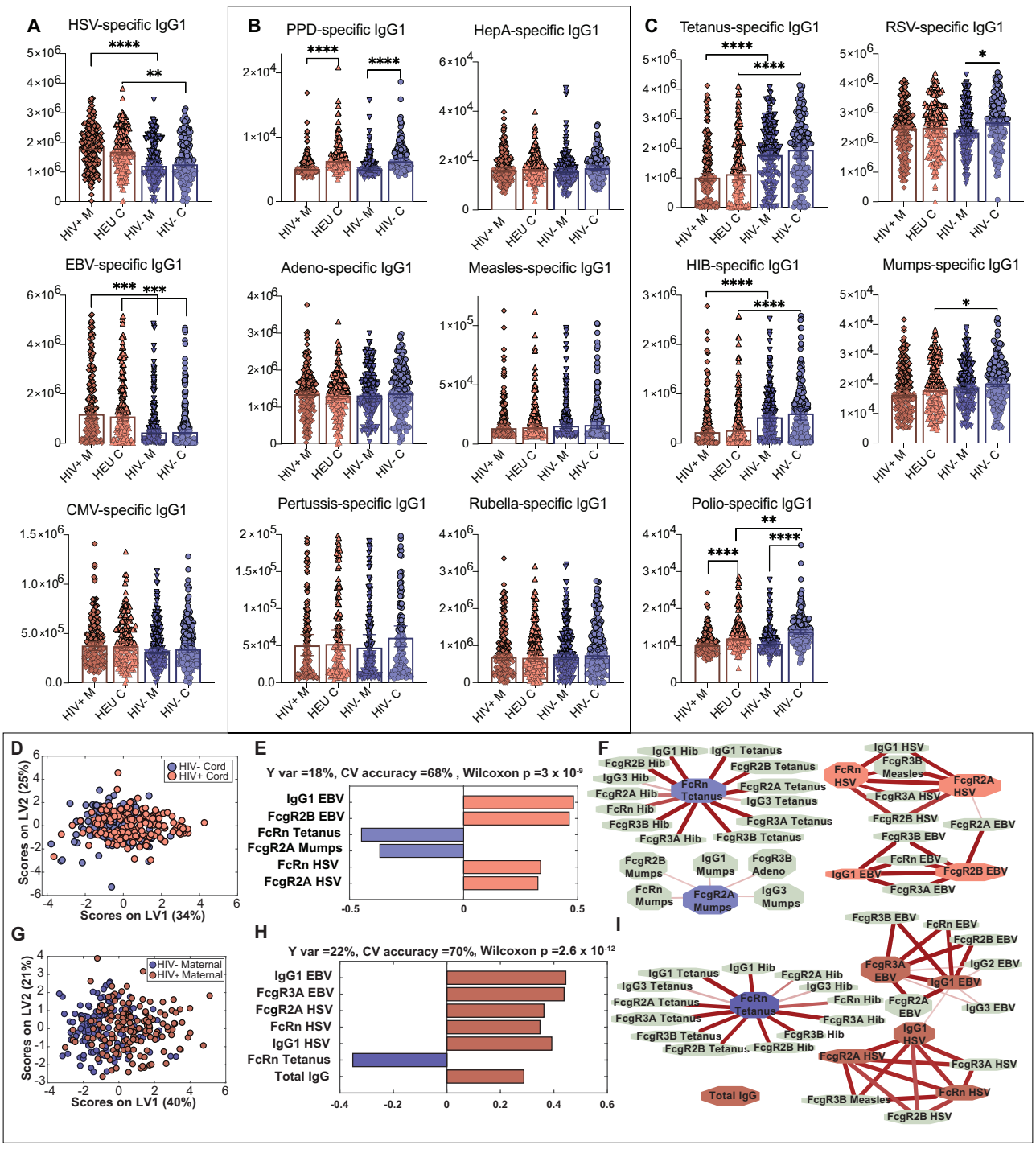

Figure 2. Differences in human immunodeficiency virus (HIV)–exposed and -unexposed umbilical cord antibody profiles are associated with differences in maternal antibody profiles. *A–C*, Univariate plots comparing immunoglobulin G1 (IgG1) levels across 4 groups of maternal and umbilical cord samples. HIV$^+$ M indicates maternal plasma from women with HIV (WHIV), HIV$^-$ M indicates HIV-uninfected maternal plasma, HEU C indicates HIV-exposed umbilical cord plasma, and HIV$^-$ C indicates HIV-unexposed umbilical cord plasma. Only significant comparisons are depicted. Maternal and umbilical cord samples were only compared within serostatus group. To assess significance of the IgG1 level differences between groups, Kruskal-Wallis nonparametric test was applied, followed by Dunn test to correct for multiple comparisons. Adjusted *P* values: *$P < .0332$, **$P < .0021$, ***$P < .0002$, ****$P < .0001$. *A*, Univariate plots showing IgG1 levels for antigen specificities where HIV-uninfected/unexposed maternal and umbilical cord plasma samples are lower than WHIV/HIV-exposed umbilical cord levels for herpesvirus antigens (chronic maternal infections). Herpes simplex virus (HSV)– and Epstein-Barr virus (EBV)–specific IgG1 levels are significantly lower in HIV-uninfected/exposed than WHIV/HIV-exposed, and cytomegalovirus-specific IgG1 differences are not statistically significant. *B*, Antigen-specific IgG1 levels that are unaffected by maternal HIV serostatus. *C*, Antigen-specific IgG1 levels that are significantly higher in the HIV-uninfected/unexposed groups than WHIV/HIV-exposed include vaccine-induced antibodies to tetanus, *Haemophilus influenzae* type b (Hib), and mumps, and nonsignificantly higher for respiratory syncytial virus and polio. *D–I*, Multivariate analysis to distinguish HIV-exposed and unexposed umbilical cord (*D–F*) and maternal (*G–I*) antibody profiles. *D*, Score plot for the orthogonalized partial least squares discriminant analysis (OPLSDA) analysis using 6 least absolute shrinkage and selection operator (LASSO)–selected features depicts moderately different profiles between HIV-exposed and -unexposed umbilical cord plasma. Latent variable 1 (LV1) captures the separation

in viremic WHIV than HIV-uninfected women, but not between nonviremic WHIV and HIV-uninfected women, nor in umbilical cord blood by maternal HIV serostatus or viremia (Figure 4C). Maternal total IgG levels and antigen-specific IgG1 transfer ratios were significantly negatively correlated with lower transfer ratios for 13 of 14 (92%) specific antigens (Figure 4D).

Finally, to further distinguish maternal antibody profiles in maternal HIV serostatus and viremia groups, we performed PLSDA on the combined set of LASSO-selected features separating each pair of groups (Figure 4E). The most striking separation was observed between HIV-uninfected women and viremic WHIV (CV accuracy = 77%). Total IgG, EBV-specific IgG1, HSV-specific IgG1, tetanus FcRn, Hib FcγR2a, and mumps FcγR2a were key features separating groups (Supplementary Figure 3*A* and 3*B*). These analyses demonstrated that viremia in WHIV and expanded herpesvirus plasma responses likely act synergistically to enhance transplacental transfer of chronic herpesvirus antibodies, potentially blocking transfer of antibodies more relevant to protecting HEU neonates against early-life pathogens.

DISCUSSION

Significant controversy remains over the origin of increased infection risk and severity in HEU infants. Prior studies of transplacental antibody transfer to HEUs report conflicting results, with some describing lower quantities of antigen-specific antibodies against Hib, influenza A, RSV, tetanus, and measles, while others found higher quantities or no difference [5–8]. However, no studies comprehensively evaluated multiple antigens simultaneously or large cohorts living in resource-limited settings. Here, we used systems serology to comprehensively analyze the landscape of transplacentally transferred antibodies in a large sub-Saharan African cohort. We demonstrate similar overall transplacental antibody transfer patterns between WHIV taking ART and HIV-uninfected comparators and efficient (umbilical cord:maternal ratio >1) transplacental antibody transfer in WHIV taking ART, suggesting intact placental function.

Concerningly, we describe altered WHIV plasma antibody profiles characterized by reduced vaccine-associated antibodies and a herpesvirus-associated inflammatory state skewing transplacental antibody transfer toward chronic herpesviruses-specific antibodies. In WHIV, herpesvirus antibodies likely saturate placental receptors, outcompeting Hib, tetanus, and mumps antibodies more important for HEU infant protection. Altered maternal antibody profiles and high total IgG observed in this relatively healthy WHIV population suggests perturbed immunity, possibly resulting from irreparable host B- and T-cell repertoire changes shifting the inflammatory balance [29] and only partially remedied by ART. In the setting of hypergammaglobulinemia, placental mechanisms regulate total IgG transfer, reducing antigen-specific antibody transfer to umbilical cord blood. Our findings suggest that adverse HEU health outcomes are driven, in part, by relatively lower antibody quality and functionality in WHIV resulting in transplacental transfer of a skewed antibody pool to the neonate, with ratios largely reflecting maternal plasma concentrations.

These findings reveal a critical opportunity to rebalance transplacental antibody transfer through selectively boosting critically important antigen-specific antibodies in WHIV. Our findings suggest that maternal boosters against Hib, mumps, and other key vaccine-preventable pathogens should be given to reproductive-age WHIV with low titers, especially those with detectable viremia and lower CD4 counts, as low maternal titers are associated with increased infant infection risk [30]. Future research should evaluate whether booster vaccination could induce higher titers of key antibodies, diluting the pool of maternal herpesvirus antibodies, outcompeting them for transplacental transfer, and enhancing transfer of antibodies most relevant to early-life protection.

Unlike others, we did not find decreased transplacental measles [6], RSV [31], or pertussis [7] IgG1 transfer in WHIV. Our findings also differ from those of Goetghebuer et al [32]. who reported differences in umbilical cord plasma in WHIV largely driven by postconception ART initiation. In our cohort, seroprofiles of WHIV initiating ART preconception differed significantly from HIV-uninfected women. This contrast could result from differences in study population. Though 82% of the Belgian WHIV were of sub-Saharan African origin, they lived in Belgium and likely had different vaccination histories and environmental exposures than our Ugandan

between HIV-exposed and HIV-unexposed cord plasma (Y var = 18% and X var = 34%), where latent variable 2 (LV2) captures the variance in antibody profiles that does not contribute to this separation (Y var = 0% and X var = 25%). *E*, Bar graph depicts loadings on LV1 ordered according to their variable importance in projection (VIP) scores and is color-coded to emphasize the features enriched in each group. *F*, Correlates of the LASSO-selected features are depicted in network format. Only correlation coefficients with multiple comparison corrected *P* values <.05 and Spearman correlation coefficients >0.3 are included. Line widths and color intensities are proportional to the correlation coefficients. Overall, higher EBV- and HSV-specific antibody titers and associated Fc receptor binding capacity are observed in HIV-exposed umbilical cord plasma, while tetanus-, Hib-, and mumps-specific antibodies are enriched in HIV-unexposed group. *G*, Similarly, OPLSDA models were built using 7 LASSO-selected antibody features. The dots in the score plot represent WHIV and HIV-uninfected maternal samples. LV1 captures the separation between these maternal groups (Y var = 22% and X var = 40%), and LV2 captures the variance in antibody profiles that does not contribute to this separation (Y var = 0% and X var = 21%). *H*, Bar graph depicts loadings on LV1 ordered according to their VIP scores and color-coded to emphasize the features enriched in each group. *I*, Correlates of the LASSO-selected features are depicted in network format with criteria and line depictions similar to (*F*). Abbreviations: CMV, cytomegalovirus; CV, cross-validation; EBV, Epstein-Barr virus; FcR, Fc receptor; HepA, hepatitis A; HEU, human immunodeficiency virus exposed, uninfected; Hib, *Haemophilus influenzae* type b; HIV, human immunodeficiency virus; HSV, herpes simplex virus; IgG, immunoglobulin G; LV, latent variable; PPD, purified protein derivative; RSV, respiratory syncytial virus.

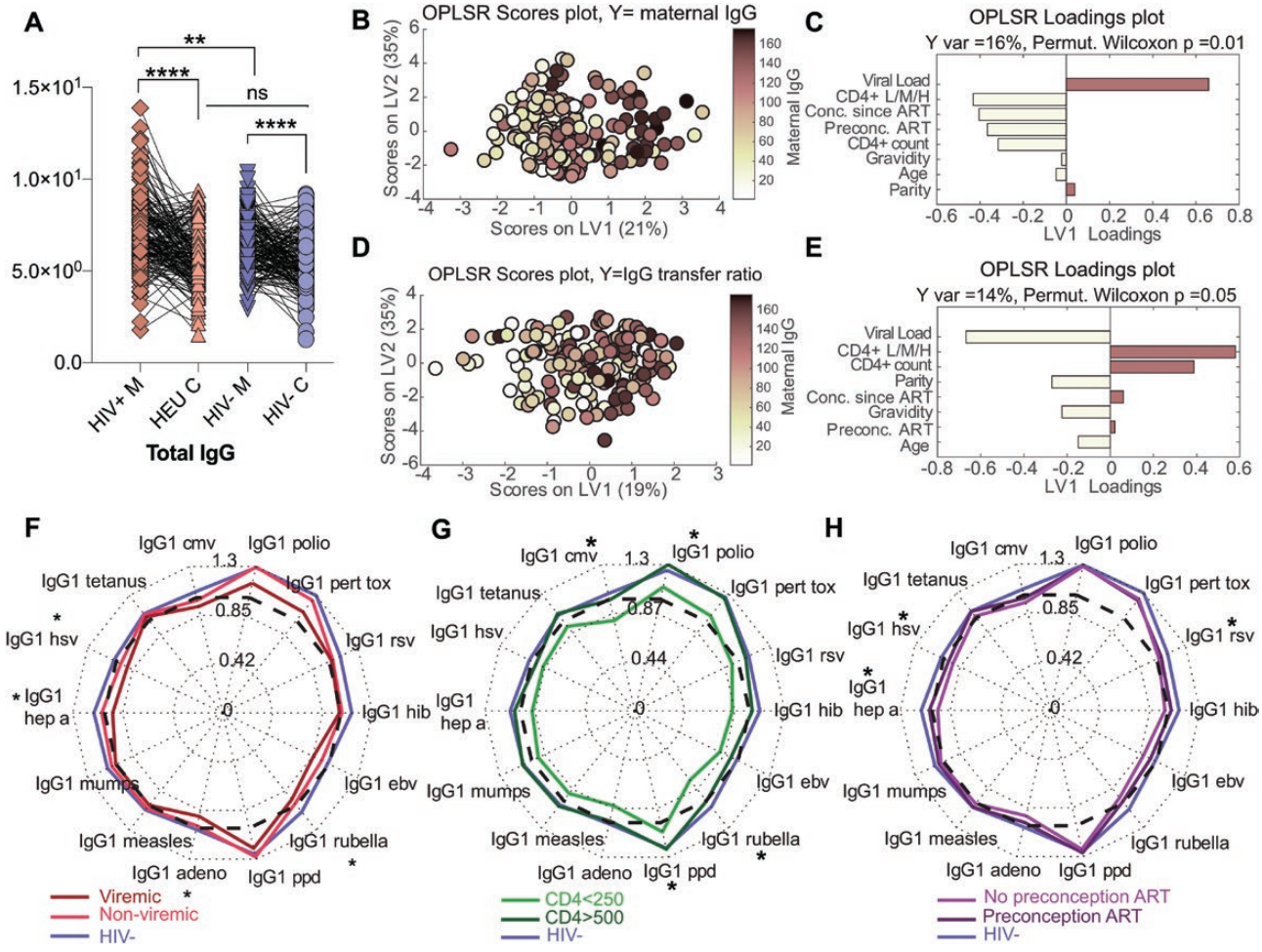

Figure 3. High viral load, low CD4 T-cell count, and time on antiretroviral therapy (ART) are determinants of high maternal total immunoglobulin G (IgG) levels and low transplacental IgG1 transfer. *A*, The dot-line plots show total IgG levels across paired mother:umbilical cord samples for human immunodeficiency virus (HIV)–infected/exposed (HIV^+) and HIV-uninfected/unexposed (HIV^-) maternal (M) and umbilical cord (C) groups. Significance was evaluated by a Kruskal-Wallis test corrected for multiple comparisons using a Dunn test, where adjusted $P < .033$ was considered significant. *$P < .033$, **$P < .0021$, ****$P < .0001$. *B–E*, Multivariate analysis to identify features associated with high maternal total IgG (*B–C*) and high total IgG transplacental transfer ratio (*D–E*). *B*, An orthogonalized partial least squares discriminant analysis (OPLSR) model was developed to define maternal features associated with total IgG titer among women with HIV (WHIV). The dots represent individual WHIV and are colored based on their rank of transplacental antibody transfer (dark = high, light = low). High IgG transfer correlates were captured on latent variable 1 (LV1), explaining 16% of the variance of IgG titer rank. This model outperformed 99% of random models (cross-validation [CV] Wilcoxon $P = .01$) *C*, Bar graph depicting the loading plot associated with total maternal IgG, in which all maternal features were ranked based on their variable importance in projection (VIP) score measuring their contribution to total IgG variance. The top 3 features have VIP score >1, signifying greater than average contribution to the variation of total IgG. *D*, A second OPLSR model was constructed to define the maternal features associated with enhanced total IgG transfer across the placenta to umbilical cord plasma. Dots represent single maternal:umbilical cord pairs colored according to their rank of high to low total IgG transfer ratio (dark = high, light = low). Features associated with highest transfer ratio are captured on LV1, accounting for 14% of the variance of IgG transfer. This model outperformed 95% of random models (CV Wilcoxon $P = .05$). *E*, Bar graph depicts the loading plot for LV1. Predictors are ranked based on their VIP score, importance in driving antibody transfer. The top 2 features, HIV viral load and CD4 L/M/H, have VIP score >1, signifying greater than average contribution to the model prediction of transplacental IgG transfer. CD4 L/M/H: $CD4^+$ T-cell counts discretized to have value 0 for CD4 <250 cells/μL (L), value 1 for CD4 250–500 cells/μL (M), and value 2 for CD4 >500 cells/μL (H). *F–H*, Radar plots of median antigen-specific transplacental IgG1 transfer ratios, homing in on the relationship between maternal HIV features and transfer ratios. *F*, Comparing median transfer ratios among 3 maternal groups: HIV-infected viremic, HIV-infected nonviremic, and HIV-uninfected. Statistical significance was tested using Wilcoxon rank-sum test between HIV-uninfected and the HIV-infected viremic groups. *G*, Comparing median transfer ratios according to maternal CD4 count groups. Statistical significance was tested using Wilcoxon rank-sum test between HIV-uninfected women and WHIV with CD4 <250 cells/μL. *H*, Comparing median transfer ratios, grouped by ART duration: between HIV-uninfected women, WHIV taking ART at conception, and WHIV not taking ART at conception. Statistical significance was tested using Wilcoxon rank-sum test between HIV-uninfected women and WHIV not taking ART preconception. *F–H*, Significance levels were corrected for multiple comparisons using Bonferroni correction across the 14 antigen specificities per panel. Adjusted *P* values < .05 are indicated with an asterisk. Abbreviations: adeno, adenovirus; ART, antiretroviral therapy; CMV, cytomegalovirus; EBV, Epstein-Barr virus; HepA, hepatitis A; HEU, HIV exposed, uninfected; Hib, *Haemophilus influenzae* type b; HIV, human immunodeficiency virus; HSV, herpes simplex virus; IgG, immunoglobulin G; LV, latent variable; ns, not significant; OPLSR, orthogonalized partial least squares discriminant analysis; pert tox, pertussis toxin; PPD, purified protein derivative; RSV, respiratory syncytial virus.

cohort [32]. Differences in social determinants of health, maternal microbiomes, nutrition, and coinfections could also contribute. Limitations of our study include lack of infant longitudinal follow-up and inability to adjust for nutritional, socioeconomic, and other potential factors influencing maternal seroprofiles.

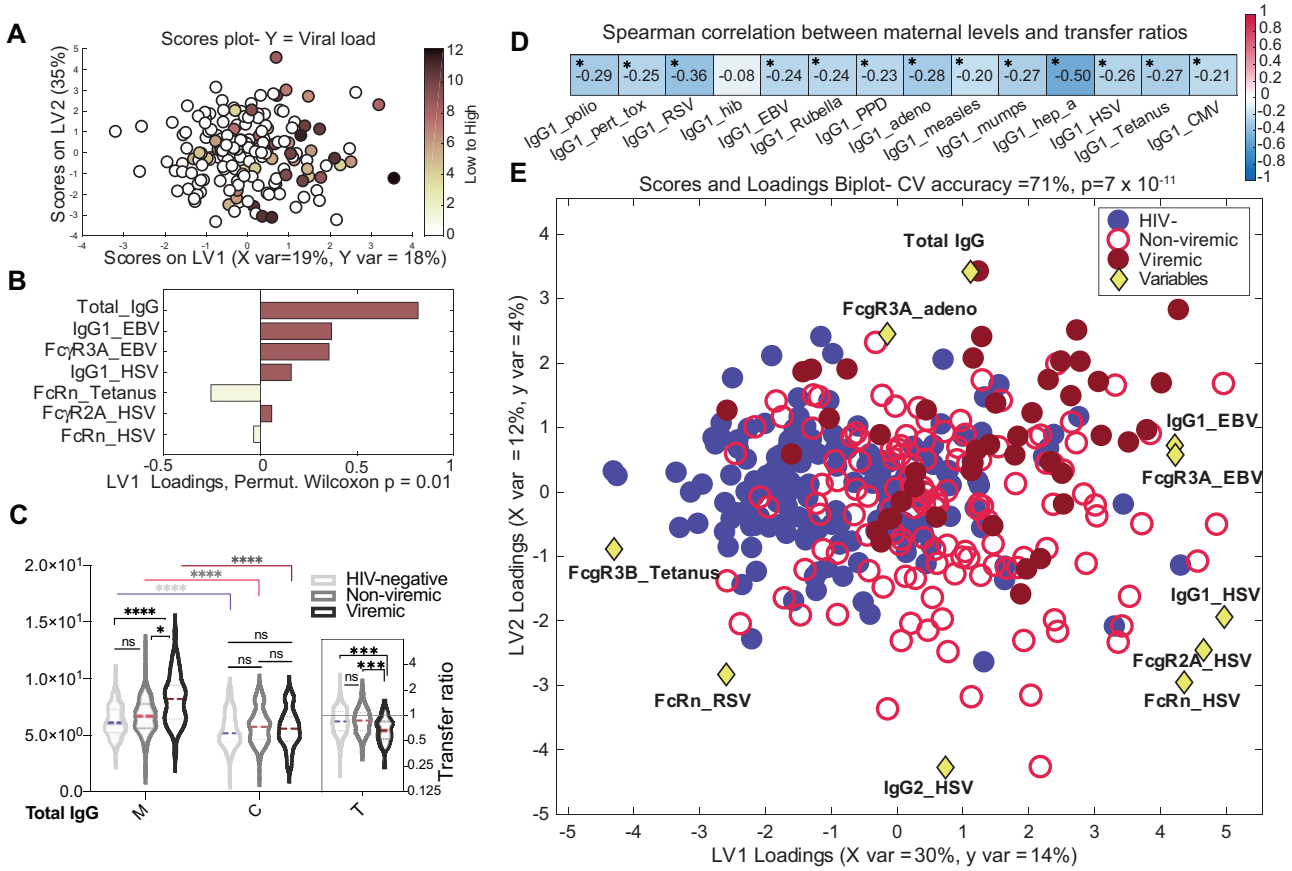

Figure 4. The contribution of maternal human immunodeficiency virus (HIV) viremia to perturbed maternal antibody profiles. *A* and *B*, Multivariate analysis to identify maternal antibody features associated with high maternal HIV viral load. *A*, Features predictive of maternal HIV viral load defined using orthogonalized partial least squares discriminant analysis model. Dots represent individual women with HIV (WHIV) and are colored based on HIV viral load (darker = higher, colorless = undetectable). Correlates of high HIV viral load are captured on latent variable 1 (LV1), explaining 18% of the variance in viral load. This model outperformed >99% of random models (cross-validation [CV] Wilcoxon $P = .008$). *B*, Bar graph depicting the loading plot associated with maternal HIV viral load, where maternal antibody and receptor features were ranked based on their variable importance in projection (VIP) score, representing each feature's contribution to viral load. Total immunoglobulin G (IgG) is the only feature with VIP score >1, signifying greater than average contribution to the variation in viral load. *C*, Violin plots show the distribution of total IgG in maternal (M) and umbilical cord (C) plasma grouped by maternal viremia status. The inset (T) depicts total IgG transfer ratios. Significance was evaluated by a Kruskal-Wallis test corrected for multiple comparisons using a Dunn test, where adjusted $P < .033$ was considered significant. $^{*}P < .033$, $^{***}P < .0002$, $^{****}P < .0001$. *D*, Spearman correlation of maternal plasma levels with corresponding transplacental transfer ratios for 14 antigen-specific IgG1 levels, calculated across all participants. False discovery rate–adjusted *P* values. $^{*}P < .05$ was considered significant. *E*, Multivariate analysis of maternal features associated with HIV viremia. Using the combined set of 12 features that separated pairwise profiles of HIV-uninfected, nonviremic WHIV, and viremic WHIV, a 3-way partial least squares discriminant analysis (PLSDA) summarizing the comparison of HIV-uninfected (n = 173, blue filled circles), nonviremic WHIV (n = 131, red open circles), and viremic WHIV (n = 45, dark red filled circles) individuals. The PLSDA biplot depicts score plots of individuals color-coded based on their HIV serostatus and HIV viremia group, which was overlaid on the 2-dimensional loading plots of the 12 input features (yellow diamonds). LV1 accounts for 30% of variance in X and 14% of variance in Y, whereas latent variable 2 explains 12% X variance and 4% Y variance. Five-fold cross validation resulted in 70% CV accuracy. Permutation testing results showed that this model significantly outperformed models based on shuffled group labels (Wilcoxon $P < 10^{-10}$). This biplot could be interpreted as the yellow diamonds "pulling" individual participants in their respective directions. Abbreviations: adeno, adenovirus; CV, cross-validation; EBV, Epstein-Barr virus; FcR, Fc receptor; HIV, human immunodeficiency virus; HSV, herpes simplex virus; IgG, immunoglobulin G; LV, latent variable; ns, not significant; RSV, respiratory syncytial virus.

Further research should focus on mechanisms causing differing immune responses in WHIV, evaluation of the efficacy of targeted vaccination to augment maternal and neonatal immunity, and longitudinal infant follow-up to measure infection risk. Ultimately, rebalancing maternal seroprofiles in WHIV is a first important step in helping HEU children battle the world of pathogens awaiting them after birth.

Supplementary Data

Supplementary materials are available at *Clinical Infectious Diseases* online. Consisting of data provided by the authors to benefit the reader, the posted materials are not copyedited and are the sole responsibility of the authors, so questions or comments should be addressed to the corresponding author.

Notes

Author contributions. S. D.: Data curation, formal analysis, investigation, methodology, validation, visualization, writing—original draft, writing—review and editing. A. L. B.: Data curation, formal analysis, validation, writing—original draft, writing—review and editing. M. J. S.: Conceptualization, funding acquisition, investigation, methodology, supervision, validation, writing—review and editing. J. N.: Conceptualization, data curation, investigation, methodology, project administration, supervision, writing—review and editing. A. G. E. and C. A.: Conceptualization,

writing—review and editing. J. A.: Data curation, investigation, supervision, writing—review and editing. M. F. J.: Conceptualization, data curation, formal analysis, investigation, methodology, validation, visualization, writing—review and editing. I. V. B.: Conceptualization, funding acquisition, investigation, methodology, supervision, validation, writing—review and editing. D. J. R.: Conceptualization, data curation, formal analysis, investigation, supervision, writing—review and editing. D. A. L.: Conceptualization, formal analysis, methodology, supervision, validation, visualization, writing—review and editing. G. A.: Conceptualization, funding acquisition, methodology, resources, writing—review and editing. L. M. B.: Conceptualization, data curation, formal analysis, funding acquisition, investigation, methodology, project administration, resources, software, supervision, validation, visualization, writing—original draft, writing—review and editing.

Acknowledgments. The authors are grateful to the cohort participants and to the Mbarara Regional Referral Hospital Maternity Staff, Mbarara University of Science and Technology, Mbarara University of Science and Technology Pathology Laboratory, and Mbarara Regional Referral Hospital Immune Suppression Syndrome Clinic for their partnership in this research.

Data sharing. Data collected for the study, including individual participant data and a data dictionary defining each field in the set, will be made available to others as de-identified participant data from the investigators on request after publication. The study protocol will also be available on request after publication. Those requesting access to data should email Dr Lisa Bebell, corresponding author, at lbebell@mgh.harvard.edu to create a data access agreement, which must be fully executed before any study data or materials can be shared.

Disclaimer. The sponsors had no role in study design, data collection, analysis or interpretation, writing the report, or decision to submit the article for publication. The content is solely the responsibility of the authors and does not necessarily represent the official views of Harvard Catalyst, Harvard University or its affiliated academic healthcare centers, the National Institutes of Health (NIH), or other funders.

Financial support. This work was supported by the Harvard University Center for AIDS Research, NIH/National Institute of Allergy and Infectious Diseases (NIAID) (grant number P30AI060354 to L. M. B.); by a KL2/Catalyst Medical Research Investigator Training award from Harvard Catalyst /Harvard Clinical and Translational Science Center (grant number KL2TR002542 to L. M. B.); the Charles H. Hood Foundation (to L. M. B.); a career development award from NIAID (grant number K23AI138856 to L. M. B.); an NIH midcareer mentoring award (grant number K24AI141036 to I. V. B.); the Weissman Family Massachusetts General Hospital (MGH) Research Scholar Award (to I. V. B.); the American Society of Tropical Medicine and Hygiene Burroughs Wellcome Postdoctoral Fellowship in Tropical Infectious Diseases (to L. M. B.); National Institutes of Health awards 3R37AI080289-11S1, R01AI146785, U19AI42790-01, U19AI135995-02, 1U01CA260476-01, and CIVIC75N93019C00052 (all to G. A.); the Bill & Melinda Gates Foundation (to G. A.); and the Musk Foundation (to G. A.).

Potential conflicts of interest. G. A. reports grants or contracts from the Ragon Institute and the MGH Scholars Program; has received consulting fees from Sanofi Pasteur and payment or honoraria for lectures from Princeton University, George Washington University, Johns Hopkins University, Washington University, University of Washington, Yale University, Walter Reed Medical Institute, State University of New York (Upstate), and Mount Sinai; holds patents on direct expression of antibodies (Novartis) (PAT056060-EP-EPA), antigen-specific antibody glycosylation as a diagnostic marker of disease state (MGH21944), system and method for the multiplexed affinity purification of proteins and cells (MIT 16927), and a rapid Fc-enhancing screening approach (MGH in preparation 2021; pending); participates on a data and safety monitoring board for a CAPRISA monoclonal therapeutic trial for the University of KwaZulu-Natal, South Africa; and has stock options with Systems Seromyx and Leyden Labs. D. J. R. reports author royalties from UpToDate and Cambridge University Press; honoraria for lectures from various academic organizations; academic support for traveling from her institution; and a pending patent for an ex vivo dual perfusion placental chamber magnetic resonance imaging compatible. All other authors report no potential conflicts.

All authors have submitted the ICMJE Form for Disclosure of Potential Conflicts of Interest. Conflicts that the editors consider relevant to the content of the manuscript have been disclosed.

REFERENCES

1. Cotton MF, Slogrove A, Rabie H. Infections in HIV-exposed uninfected children with focus on sub-Saharan Africa. Pediatr Infect Dis J **2014**; 33:1085–6.
2. Slogrove A, Reikie B, Naidoo S, et al. HIV-exposed uninfected infants are at increased risk for severe infections in the first year of life. J Trop Pediatr **2012**; 58:505–8.
3. Labuda SM, Huo Y, Kacanek D, et al. Rates of hospitalization and infection-related hospitalization among HIV-exposed uninfected children compared to HIV-unexposed uninfected children in the United States, 2007–2016. Clin Infect Dis **2020**; 71:332–9.
4. Brennan AT, Bonawitz R, Gill CJ, et al. A meta-analysis assessing all-cause mortality in HIV-exposed uninfected compared with HIV-unexposed uninfected infants and children. AIDS **2016**; 30:2351–60.
5. Ho A, Mapurisa G, Madanitsa M, et al. Impact of maternal HIV infection and placental malaria on the transplacental transfer of influenza antibodies in mother–infant pairs in Malawi, 2013–2014. Open Forum Infect Dis **2019**; 6:ofz383.
6. Jallow S, Cutland CL, Masbou AK, Adrian P, Madhi SA. Maternal HIV infection associated with reduced transplacental transfer of measles antibodies and increased susceptibility to disease. J Clin Virol **2017**; 94:50–6.
7. Jones CE, Naidoo S, De Beer C, Esser M, Kampmann B, Hesseling AC. Maternal HIV infection and antibody responses against vaccine-preventable diseases in uninfected infants. JAMA **2011**; 305:576–84.
8. Weinberg A, Mussi-Pinhata MM, Yu Q, et al. Excess respiratory viral infections and low antibody responses among HIV-exposed, uninfected infants. AIDS **2017**; 31:669–79.
9. Wabwire-Mangen F, Gray RH, Mmiro FA, et al. Placental membrane inflammation and risks of maternal-to-child transmission of HIV-1 in Uganda. J Acquir Immune Defic Syndr **1999**; 22:379–85.
10. Schwartz DA, Sungkarat S, Shaffer N, et al. Placental abnormalities associated with human immunodeficiency virus type 1 infection and perinatal transmission in Bangkok, Thailand. J Infect Dis **2000**; 182:1652–7.
11. Jauniaux E, Nessmann C, Imbert MC, Meuris S, Puissant F, Hustin J. Morphological aspects of the placenta in HIV pregnancies. Placenta **1988**; 9:633–42.
12. D'Costa GF, Khadke K, Patil YV. Pathology of placenta in HIV infection. Indian J Pathol Microbiol **2007**; 50:515–9.
13. de Moraes-Pinto MI, Verhoeff F, Chimsuku L, et al. Placental antibody transfer: influence of maternal HIV infection and placental malaria. Arch Dis Child Fetal Neonatal Ed **1998**; 79:F202–5.
14. Wilcox CR, Holder B, Jones CE. Factors affecting the FcRn-mediated transplacental transfer of antibodies and implications for vaccination in pregnancy. Front Immunol **2017**; 8:1294.
15. Bebell LM, Siedner MJ, Ngonzi J, et al. Brief report: chronic placental inflammation among women living with HIV in Uganda. J Acquir Immune Defic Syndr **2020**; 85:320–4.
16. Bebell LM, Parks K, Le MH, et al. Placental decidual arteriopathy and vascular endothelial growth factor A (VEGF-A) expression among women with and without HIV. J Infect Dis **2021**; 224:S694–700.
17. Brown EP, Licht AF, Dugast AS, et al. High-throughput, multiplexed IgG subclassing of antigen-specific antibodies from clinical samples. J Immunol Methods **2012**; 386:117–23.
18. Brown EP, Dowell KG, Boesch AW, et al. Multiplexed Fc array for evaluation of antigen-specific antibody effector profiles. J Immunol Methods **2017**; 443:33–44.
19. Chung AW, Kumar MP, Arnold KB, et al. Dissecting polyclonal vaccine-induced humoral immunity against HIV using systems serology. Cell **2015**; 163:988–98.
20. Lau KS, Juchheim AM, Cavaliere KR, Philips SR, Lauffenburger DA, Haigis KM. In vivo systems analysis identifies spatial and temporal aspects of the modulation of TNF-α-induced apoptosis and proliferation by MAPKs. Sci Signal **2011**; 4:ra16–ra.
21. Chong I-G, Jun C-H. Performance of some variable selection methods when multicollinearity is present. Chemometr Intell Lab Syst **2005**; 78:103–12.
22. Jennewein MF, Goldfarb I, Dolatshahi S, et al. Fc glycan-mediated regulation of placental antibody transfer. Cell **2019**; 178:202–15.e14.
23. Westerhuis JA, van Velzen EJJ, Hoefsloot HCJ, Smilde AK. Multivariate paired data analysis: multilevel PLSDA versus OPLSDA. Metabolomics **2010**; 6:119–28.
24. Garty BZ, Ludomirsky A, Danon YL, Peter JB, Douglas SD. Placental transfer of immunoglobulin G subclasses. Clin Diagn Lab Immunol **1994**; 1:667–9.
25. Clements T, Rice TF, Vamvakas G, et al. Update on transplacental transfer of IgG subclasses: impact of maternal and fetal factors. Front Immunol **2020**; 11:1920.

26. van Erp EA, Luytjes W, Ferwerda G, van Kasteren PB. Fc-mediated antibody effector functions during respiratory syncytial virus infection and disease. Front Immunol **2019**; 10:548.
27. Martinez DR, Fong Y, Li SH, et al. Fc characteristics mediate selective placental transfer of IgG in HIV-infected women. Cell **2019**; 178:190–201.e11.
28. Atwell JE, Thumar B, Formica MA, et al. Hypergammaglobulinemia and impaired transplacental transfer of respiratory syncytial virus antibody in Papua New Guinea. Pediatr Infect Dis J **2019**; 38:e199–202.
29. Kazer SW, Walker BD, Shalek AK. Evolution and diversity of immune responses during acute HIV infection. Immunity **2020**; 53:908–24.
30. Brooks JI, Bell CA, Rotondo J, et al. Low levels of detectable pertussis antibody among a large cohort of pregnant women in Canada. Vaccine **2018**; 36:6138–43.
31. Patel SM, Jallow S, Boiditswe S, et al. Placental transfer of respiratory syncytial virus antibody among HIV-exposed, uninfected infants. J Pediatr Infect Dis Soc **2019**; 9:349–56.
32. Goetghebuer T, Smolen KK, Adler C, et al. Initiation of antiretroviral therapy before pregnancy reduces the risk of infection-related hospitalization in human immunodeficiency virus-exposed uninfected infants born in a high-income country. Clin Infect Dis **2019**; 68:1193–203.